International Journal of Pharmaceutics 590 (2020) 119917

Contents lists available at ScienceDirect

International Journal of Pharmaceutics

journal homepage: www.elsevier.com/locate/ijpharm

Fabrication of biodegradable particles with tunable morphologies by the addition of resveratrol to oil in water emulsions

Christopher Isely [a], Alexandra C. Stevens [b], Gregory L. Tate [a], John R. Monnier [a], R. Michael Gower [a,b,*]

[a] Department of Chemical Engineering, University of South Carolina, Columbia, SC 29208, USA
[b] Biomedical Engineering Program, University of South Carolina, Columbia, SC 29208, USA

ARTICLE INFO

Keywords:
Biomaterials
Resveratrol
Emulsion
Nonspherical particles

ABSTRACT

Particles for biomedical applications can be produced by emulsifying biocompatible polymers dissolved in an organic solvent in water. The emulsion is then transferred to an extraction bath that removes the solvent from the dispersed droplets, which leads to polymer precipitation and particle formation. Typically, the particles are smooth and spherical, likely because the droplets remain fluid throughout the solvent extraction process allowing minimization of surface area as the volume decreases. Few modifications to this technique exist that alter the spherical geometry, even though particle performance, from drug delivery to engaging cells of the body, can be tuned with morphology. Here we demonstrate that incorporation of resveratrol, with the aid of ethanol, into the oil phase of an emulsion of poly(lactide-co-glycolide) and dichloromethane in aqueous poly(vinyl alcohol) leads to a crumpled particle morphology. Video microscopy of particle formation revealed that during solvent extraction the droplet crumples in on itself, which does not occur when only ethanol is added to the emulsion. It is unclear why this occurs with resveratrol, but its hydroxyl groups appear to be optimally positioned because removal of the 4′ hydroxyl or addition of a 3′ hydroxyl resulted in a loss of crumpled particle morphology. We demonstrate that particle morphology can be tuned from that of a crumpled sheet of paper to a deflated sphere by switching out ethanol for a different cosolvent. We quantify the degree of particle deformation with surface area calculated from krypton adsorption isotherms and BET theory and find surface area correlates with resveratrol loading in the particle. Furthermore, spherical particles are achieved when ethyl acetate is used in lieu of dichloromethane and a cosolvent. We propose that during solvent extraction, resveratrol accumulates at the droplet surface where it inhibits polymer chain motion necessary to maintain a spherical geometry and the role of cosolvent is to redistribute resveratrol from the droplet bulk to its surface. This method of producing nonspherical particles extends to polycaprolactone and poly(L-lactic acid) and is compatible with the encapsulation of a hydrophobic fluorescent dye, suggesting hydrophobic bioactive agents could be encapsulated. Taken together, we demonstrate an ability to control morphology of biocompatible polymer particles produced by the widely practiced oil-in-water/solvent extraction protocol via the addition of resveratrol and a cosolvent to the oil phase. The methodology reported is straight forward, and scalable, and expected to be of utility in applications in which a deviation from the default smooth, spherical morphology is desired.

1. Introduction

The oil in water (O/W) emulsion/solvent extraction technique for making biodegradable polymer particles involves dissolving a polymer in an organic solvent (typically dichloromethane, DCM) and homogenizing in an aqueous solution of an emulsifier (typically polyvinyl alcohol, PVA). The two phases are immiscible, and spherical droplets are produced because this geometry minimizes interfacial energy. The emulsion is then added to a large volume of aqueous solution and the organic solvent is extracted from the dispersed phase, which results in the polymer precipitating and hardening into particles. The particles are then recovered through centrifugation. This technique is one of the most

* Corresponding author at: Department of Chemical Engineering, University of South Carolina, Swearingen Engineering Center Room 2C21, 301 Main Street, Columbia, SC 29208, USA.
E-mail address: gowerrm@mailbox.sc.edu (R.M. Gower).

https://doi.org/10.1016/j.ijpharm.2020.119917
Received 23 June 2020; Received in revised form 18 September 2020; Accepted 21 September 2020
Available online 3 October 2020
0378-5173/Published by Elsevier B.V.

studied and utilized for producing polymer particles because of its versatility and scalability, and it is used for several FDA approved polymer-based, controlled-release therapies such as Vivitrol (Syed and Keating, 2013), Lupron Depot (Ogawa et al., 1988), and Risperdal (Su et al., 2011). The O/W emulsion/solvent extraction technique allows for tuning of many particle properties including, size, drug release rate, and surface chemistry (Li et al., 2008; Wischke and Schwendeman, 2008). However, altering particle morphology is challenging because of the tendency of this emulsion system to form spheres (Champion et al., 2007).

Tuning particle morphology is of interest because it impacts cell-material interactions and subsequent biological responses (Mitragotri, 2009). Cells interact differently with nonspherical particles than spherical ones (Champion and Mitragotri, 2006; Hussain et al., 2019; Li et al., 2016). For example, macrophages internalize ellipsoidal particles in an orientation dependent manner. The long end of the ellipsoid is internalized more readily than the flat side (Champion and Mitragotri, 2006). Additionally, fibroblasts attach more readily to particles with a wrinkled surface than those that are smooth (Li et al., 2016). Finally, nonspherical particles cause maturation of dendritic cells to a greater extent than spherical particles (Hussain et al., 2019). Particle fabrication techniques used in these studies include particle film stretching (Champion and Mitragotri, 2006), photopolymerization (Li et al., 2016), and microfluidics (Hussain et al., 2019). While these methods are elegant, they are technically challenging and do not have a history of implementation in GMP manufacturing (Lee et al., 2016; Wischke and Schwendeman, 2008). Thus, while these studies demonstrate the importance of particle morphology on the biological response, the particle fabrication techniques employed may be difficult to adapt to the pharmaceutical industry (Banerjee et al., 2016; Park et al., 2019).

The scalability of the O/W emulsion technique makes it attractive for making nonspherical particles at an industrial scale. As a point of comparison, photopolymerization and lithography produce approximately 10^6 particles per day with constant operation; in contrast, a bench-scale O/W emulsion batch process produces 10^9 particles in a matter of hours and is only limited by the size of the vessel (Champion et al., 2007). While nonspherical particles have been achieved using O/W emulsion systems (Mohamed and van der Walle, 2006), they required poloxamer surfactants that have yet to be incorporated in an FDA approved polymer particle controlled release therapy (Park et al., 2019). Taken together, a methodology to modulate particle morphology that utilizes the DCM/PVA emulsion system would be highly desirable.

Recently, we investigated poly(lactide-co-glycolide) particles for delivery of resveratrol to fat tissue, a small molecule with anti-obesity properties (Baur and Sinclair, 2006) and an established safety profile in humans (Almeida et al., 2009). To accomplish this, we developed a method to encapsulate resveratrol within the particles using the DCM/PVA emulsion system by utilizing ethanol as a cosolvent in the oil phase (Isely et al., 2019). Unexpectedly, we found that the incorporation of resveratrol into the particles led to a non-spherical morphology. While the previous study evaluated the particles for controlled release of resveratrol, an investigation into why the emulsion system produced non-spherical particles was not carried out. Herein, we sought to study the system by investigating the effect of cosolvent, primary solvent and type of stilbene on particle morphology. In addition, we investigate its applicability to additional polyesters used in FDA approved devices (Ulery et al., 2011) and demonstrate an ability to encapsulate a model hydrophobic drug, coumarin 6. Taken together, the data presents a facile method for controlling the morphology of polyester particles. Given the importance of particle morphology in cell-material interactions, our findings may aid in the field's ability to control biological responses with biocompatible particulate systems.

2. Materials and methods

2.1. Materials

75:25 poly(D,L-lactide-co-glycolide) (PLG) with a lauryl ester end group and an inherent viscosity of 0.79 dL/g and ester terminated polycaprolactone (PCL) with an inherent viscosity of 1.24 g/dL were purchased from Evonik (Birmingham, AL). Dichloromethane (DCM), resveratrol (RSV), poly(vinyl alcohol) (PVA) (MW 13,000–23,000, 87–89% hydrolyzed), poly(L-lactide) (PLLA) with an ester end group and an inherent viscosity of 1.1 dL/g, pinosylvin and coumarin 6 were purchased from Sigma (St. Louis, MO). Ethyl acetate (EA) was purchased from Macron Fine Chemicals (Center Valley, PA) and *trans*-stilbene was purchased from TCI Chemicals (Portland, OR). Piceattanol was purchased from Cayman (Ann Arbor, MI). Methanol (MeOH) and acetone were purchased from BDH Chemicals (Radnor, PA). Ethanol (ETOH) was purchased from Decon Laboratories (King of Prussia, PA). Dimethyl sulfoxide (DMSO) was purchased from Fisher (Hampton, NH). Ultrapure water was obtained from a Thermo Scientific Barnstead Nanopure system.

2.2. Polymer particle fabrication

Polymer particles were prepared using a single oil-in-water emulsification/solvent extraction method as described previously with modifications (Murphy et al., 2018). Briefly, polymer was dissolved in organic solvent at a concentration that would achieve a final organic phase concentration of 6% (wt/wt), hereafter simply "6%". If a stilbene was included, it was dissolved in cosolvent and added to the organic phase for final concentrations and cosolvent proportions listed in Table 1. For the emulsion, 0.6 mL of organic phase was added dropwise into 4 mL of an aqueous solution of 1% (wt/v) polyvinyl alcohol (PVA), hereafter simply "1%", and homogenized at 7000 rpm for 30 s using a Kinematica PT3100D homogenizer. Solvent extraction was then conducted by adding the homogenization mixture to 16 mL of ultrapure water and then stirring the mixture for 5 h. This allows the organic solvent to extract and evaporate and the resulting particles to harden. The particles were then passed through a 40 μm filter (Greiner Bio-one), collected via centrifugation at 1750xg and washed 4 times in ultrapure water. Washed particles were frozen at −20 °C and subsequently lyophilized overnight with a Labconco freeze dryer. Recovered particles were stored under vacuum in a dry environment at room temperature. For coumarin 6 loaded particles, all conditions were the same as the first formulation in Table 1, except coumarin 6 was added to the organic phase at 0.5 mg/mL.

Table 1
Conditions used for particle formulations.

Primary Solvent	Cosolvent	Stilbene	Stilbene concentration	Volume % of cosolvent	Polymer
DCM	**ETOH**	Resveratrol	10 mg/mL	25%	PLG
DCM	**MEOH**	Resveratrol	10 mg/mL	25%	PLG
DCM	**Acetone**	Resveratrol	10 mg/mL	25%	PLG
DCM	ETOH	Resveratrol	**4 mg/mL**	**25%**	PLG
DCM	ETOH	Resveratrol	**0 mg/mL**	**25%**	PLG
DCM	ETOH	Resveratrol	**4 mg/mL**	**10%**	PLG
DCM	ETOH	Resveratrol	10 mg/mL	25%	**PCL**
DCM	ETOH	Resveratrol	10 mg/mL	25%	**PLLA**
DCM	ETOH	**Piceattanol**	10 mg/mL	25%	PLG
DCM	ETOH	**Pinosylvin**	10 mg/mL	25%	PLG
DCM	ETOH	**Trans-Stilbene**	10 mg/mL	25%	PLG
EA	**None**	Resveratrol	10 mg/mL	0%	PLG

DCM: dichloromethane; EA: ethyl acetate; ETOH: ethanol; MEOH: methanol; PLG: poly(lactide-co-glycolide); PCL: polycaprolactone; PLLA: poly(L-lactide).

2.3. Video microscopy of particle formation

Particle formation was visualized under a Nikon Eclipse Ci microscope after the emulsion process had taken place. After homogenization, 10 μL of the emulsion was transferred onto a glass slide. This was then observed under the microscope while images were acquired every second for 5 min, which was a sufficiently long time that no more particle formation was observed. Videos were made with a frame rate of 10 images per second.

2.4. Powder X-ray diffraction

A Rigaku MiniFlex X-ray diffractometer with high sensitivity 1D silicon strip detector (D\teX Ultra) was used to detect the presence of crystalline structure within the particles. 10 mg of samples were spread on zero-background holders for analysis. PXRD was performed over a range of 5-80° 2θ at room temperature at a scan rate of 2°/min. An x-ray source with Cu target at 30 kV and 15 mA was used to generate Cu Kα x-rays ($\lambda = 1.54059$ Å) for analysis. Diffraction was recorded as intensity vs. 2θ. Peak fitting was performed using Fityk curve fitting program (Wojdyr, 2010).

2.5. Sessile drop

To qualitatively determine interfacial tension of the emulsion system, a sessile drop experiment of the aqueous and organic phases was employed. 4 mL of aqueous phase (1% PVA) was added to a 20 mL scintillation vial. Into this, 0.3 mL of organic phase was carefully added to the bottom of the vial. Images were then taken from a level surface and relative height and angle of contact analyzed.

2.6. Scanning Electron microscopy (SEM) and Light microscopy (LM)

Carbon adhesive tape was attached to aluminum SEM stubs, and particles were spread onto the stubs. Compressed air was applied briefly to the particles to create a monolayer on the carbon tape. Particles were sputtered with gold 3 times for 60 s in a Denton Desk II Vacuum sputter coater. Images were taken using a TESCAN Vega3 Scanning Electron Microscope at 10 kV.

Light and fluorescence microscopy images of particles were taken on an EVOS FL microscope at 20x magnification. Particles were prepared in ultrapure water and suspended at a concentration of 0.25 mg/mL. 400 μL of these suspensions was added to a well of a 48-well plate and allowed to settle prior to image acquisition. Fluorescence images were taken on the green GFP (470 nm) fluorescence setting.

2.7. Measurement of particle size

Particle size was found by analyzing light microscopy images using ImageJ software. Briefly, three representative images were taken of each particle condition and converted to binary (B/W) colors. The Particle Analysis plugin in ImageJ was used to measure particle diameter. We report the mean particle diameter and the coefficient of variation (CV %), which is the standard deviation divided by the mean. We validated this method previously (Isely et al., 2019) by accurately measuring the size of purchased polystyrene beads.

2.8. Mass yield and resveratrol loading

Mass yield was calculated by dividing the mass of recovered particles by the mass of polymer and resveratrol emulsified. Particle mass yield was calculated according to Eq. (1).

$$MassYield(\%) = \left(\frac{M_{PT}}{M_{Pol} + M_{RE}}\right) * 100 \quad (1)$$

where M_{PT} is the mass of particles recovered from the emulsion, M_{Pol} is the mass of polymer added to the emulsion, and M_{RE} is the mass of resveratrol added to the emulsion.

Resveratrol content was determined by dissolving 1 mg of particles in 1 mL DMSO and measuring absorbance at 330 nm using a Spectramax 190 UV–Vis spectrophotometer. A 10-point standard curve was prepared by dissolving 1 mg of empty particles and a known mass of resveratrol in DMSO. Resveratrol concentration was determined by comparing the unknown samples to the standard curve. Resveratrol loading (μg/mg) was calculated by dividing the mass of resveratrol extrapolated from the standard curve by the mass of particles dissolved in DMSO. Resveratrol loading was calculated by equation (2).

$$Loading\left(\frac{\mu g}{mg}\right) = \frac{M_R}{M_P} \quad (2)$$

where M_P is the mass of particles dissolved in DMSO and M_R is the mass of resveratrol measured in those particles.

2.9. Calculation of surface area

Surface area of particles was determined by the Brunauer Emmet Teller (BET) gas adsorption method (Brunauer et al., 1938) using krypton adsorption isotherms measured using a Micromeritics ASAP 2020 physisorption instrument. Approximately 250 mg of particles were weighed out in a glass sample tube and degassed for 12 h at 30 °C. Krypton adsorption measurements were then carried out at 77 K up to $P/P_0 = 0.3$. BET transformation of the Kr adsorption isotherms was fit with linear regression over appropriate range. Linear fitting of BET transform plot was considered acceptable above an R^2 of 0.999. We validated that our protocol would provide accurate, reproducible measurements by analyzing 250 mg of a low surface area silica standard (0.20 ± 0.03 m^2/g) provided by Micromeritics in three independent experiments (Table 2.) The average value for the three trials fell within the reported range of the low SA alumina standard. Surface area measurements of polymer particles were then run 1 or 2 times for each condition.

2.10. Differential centrifugation of nonspherical particles

Particles were separated by size based on the principle that large particles sediment more readily than small particles. For our system, we found that 10 min of centrifugation at 1xg sedimented 25 μm particles while 30xg sedimented 6 μm particles and 250xg sedimented 2 μm particles and smaller. We suspended 50 mg of nonspherical particles in 40 mL water in a 50 mL centrifugation tube and centrifuged at 1xg for 10 min. The supernatant was then collected and centrifuged for 10 min at 30xg. Finally, the supernatant of the second spin was centrifuged at 250xg for 10 min. This produced particles in size ranges of 2 μm – 6 μm, 6 μm – 25 μm, and 25 μm and larger. Particle sizing is described earlier in the methods.

3. Results

3.1. Observing particle formation with video microscopy

Previously, we reported that the addition of resveratrol to the oil phase of a DCM/PLG/PVA/H_2O emulsion using ethanol as co-solvent led to the formation of nonspherical particles with creased or wrinkled

Table 2
Surface area measurements of low surface area silica standard.

Trial # (Date)	BET Surface area (m^2/g)
1 (11/16/19)	0.1703 ± 0.0045
2 (11/21/19)	0.1730 ± 0.0014
3 (11/22/19)	0.1757 ± 0.0014

surfaces (Isely et al., 2019). To visualize the process by which the oil droplets become nonspherical particles, we imaged particle formation using video microscopy (Video 1, 2, 3). This was achieved by forming the emulsion and then rapidly transferring a small sample to a glass slide for observation and video recording. We found that in emulsions with resveratrol, droplets buckled and crumpled as they decreased in volume, presumably as DCM and ethanol diffuse out of the droplet. In contrast, droplets formed without resveratrol maintained spherical geometry as their volume decreased (Fig. 1). SEM images confirm that particles made with DCM or DCM and ethanol are spherical, while most particles made with resveratrol are highly crumpled (Fig. 1, fourth column). The video microscopy indicates that when resveratrol is incorporated into the emulsion, the droplet deviates from its spherical form as volume is decreased leading to a crumpled morphology.

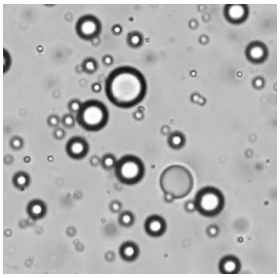

Video 1.

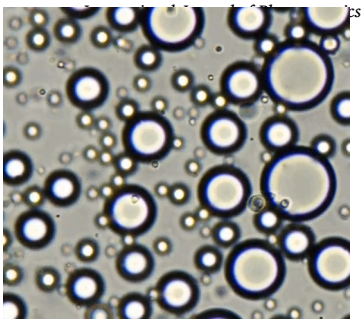

Video 2.

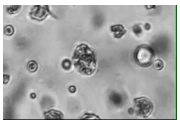

Video 3.

3.2. XRD analysis

We next sought to determine if the resveratrol was crystalline in the particles made with the small molecule. To determine this, we conducted X-ray diffraction (Fig. 2, PLG + RSV, blue line). For comparison, we also investigated free resveratrol (RSV, black line), particles made without resveratrol (PLG, orange line), and a physical mixture of the two (PLG + RSV Mixed, yellow line). Particles made with resveratrol had a loading of 65 μg/mg or 6.5%, and thus, the physical mixture was 6.5% resveratrol by mass. The diffractogram for free resveratrol indicated it was crystalline with several sharp diffraction peaks at 7.0, 16.7, 19.6 and 28.6° among others. The amorphous nature of the particles made without resveratrol was evidenced by a broad peak between 10 and 25°. The physical mixture of resveratrol and particles exhibited several diffraction peaks (including 7.1, 16.9, 19.9, 29.0°), indicating crystalline resveratrol could be detected at the weight percent used (6.5%). The diffractogram for the particles made with resveratrol exhibited peaks at 7.0, 16.8, 19.6 and 28.7°, similar to those observed in the physical

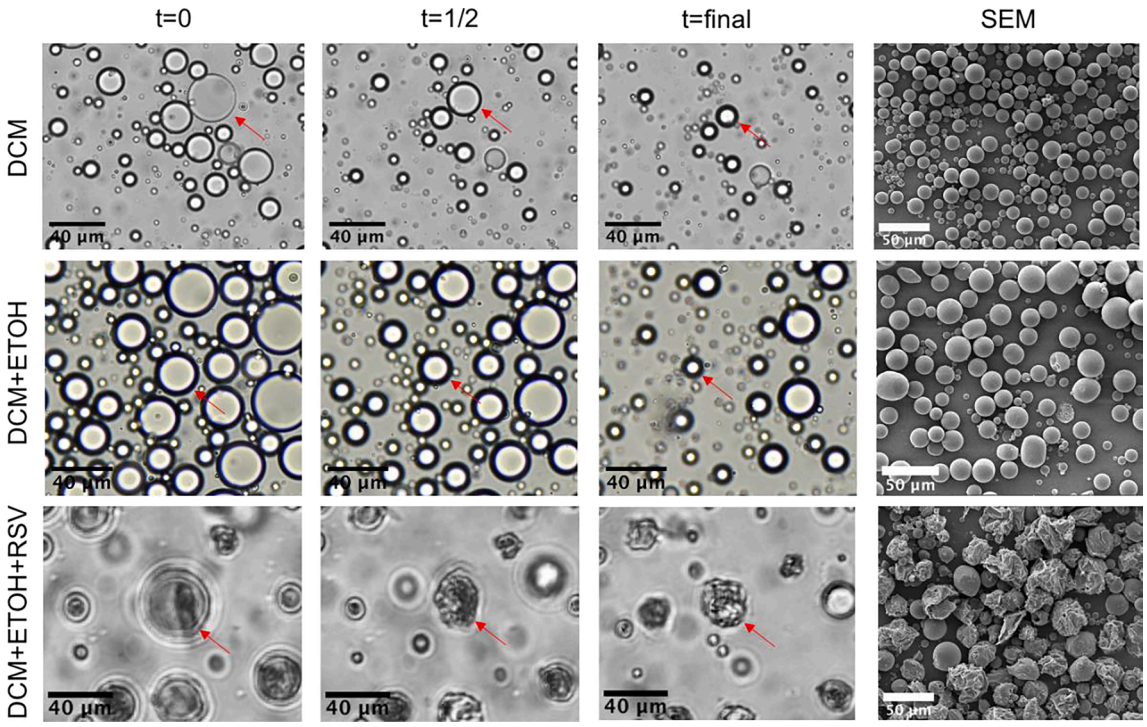

Fig. 1. Images from video microscopy of particle formation with corresponding SEM images. The results of three emulsions are shown. For all cases, the concentration of PLG in the oil phase is 6% and the concentration of PVA in the aqueous phase is 1%. The formulation of the oil phase varies by row. The top row is 100% DCM. The middle row is 75% DCM and 25% ethanol (ETOH). The bottom row is 75% DCM, 25% ETOH and 10 mg/mL resveratrol (RSV). Frames are shown from the beginning of video acquisition (t = 0), midway through the video (t = 1/2) and at the end of the video when particle size has stabilized (t = final). Red arrows indicate the same droplet over time for each condition. SEM images of the particles are shown in the right-hand column.

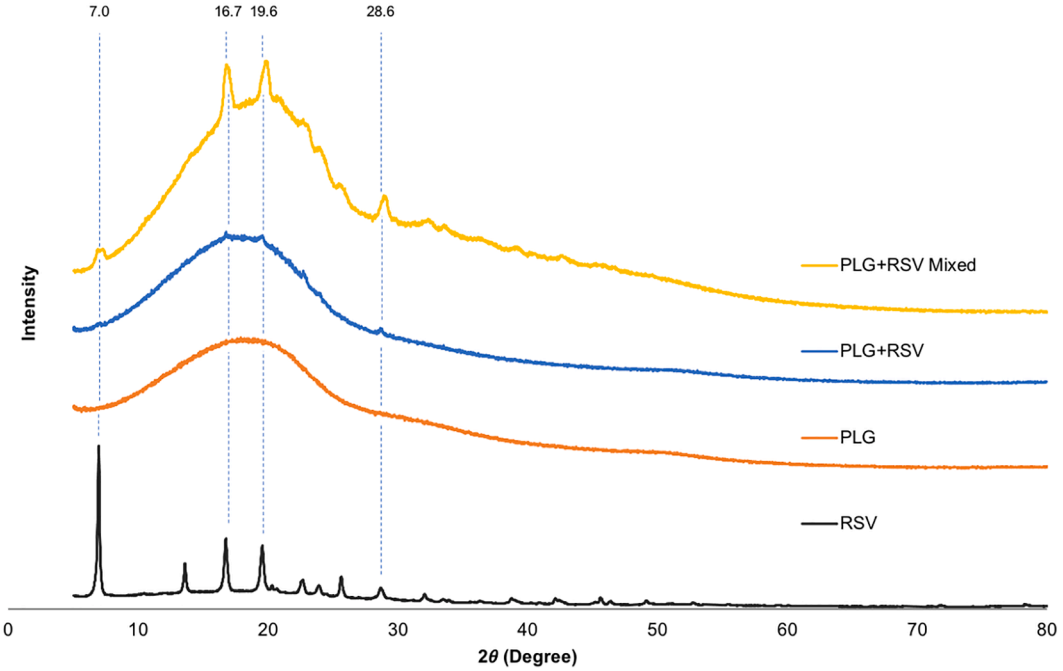

Fig. 2. X-ray diffraction. Diffractogram of free resveratrol (RSV, black curve), PLG particles (PLG, orange curve), particles made with resveratrol with a loading of 65 μg/mg (PLG + RSV, blue curve) and a physical mixture of particles and resveratrol that was 6.5% resveratrol by mass (PLG + RSV Mixed, yellow curve). Curves are displayed as Intensity vs. 2θ. Diffraction peaks shared by the particles containing resveratrol (blue curve), the physical mixture of particles and resveratrol (yellow curve,) and free resveratrol (black curve) are indicated with dotted blue lines with the corresponding 2θ measurement reported directly above the line.

mixture (albeit they were smaller). The data suggest that a small amount of the resveratrol may be crystalline in the particles made with the small molecule.

3.3. Sessile drop analysis of interfacial tension

Decreasing interfacial tension of an emulsion can lead to deviations from spherical morphology (Hussain et al., 2019; Liu et al., 2012). To determine if resveratrol was affecting interfacial tension, we employed the sessile drop method to study the shape of a drop of the organic phase in the aqueous phase. In this method, the height of the drop is directly proportional to the interfacial tension between the two phases (Rotenberg et al., 1983). Fig. 3A shows that PLG dissolved in DCM pipetted into an aqueous solution of PVA forms a sessile drop on the bottom of the vial. Fig. 3B indicates that when the organic phase (PLG + DCM) contains 25% ethanol the drop decreases in height, indicating the interfacial tension is decreased, which is consistent with another study (Rawat and Burgess, 2010). In Fig. 3C, resveratrol is added to the organic phase containing DCM, PLG and ethanol. The resveratrol can be seen diffusing into the aqueous phase as a white precipitate. The drop containing resveratrol appears to have a similar height to the drop containing only DCM and PLG (Fig. 3A), suggesting the addition of resveratrol nullifies the decrease in interfacial tension caused by the ethanol.

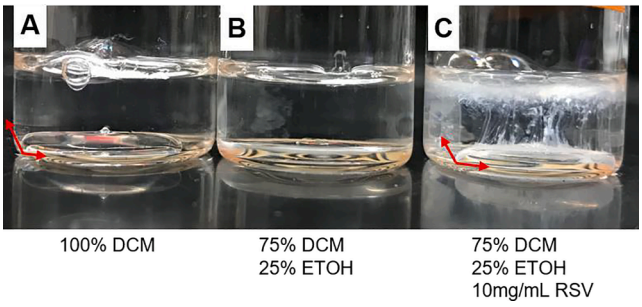

Fig. 3. Effect of ethanol and resveratrol on sessile drop formation. Image of sessile drops formed by pipetting the organic phase into aqueous solution of PVA. Aqueous phase is 1% PVA in water. The organic phase is 6% PLG dissolved in A) 100% DCM, B) 25% ethanol 75% DCM and C) 25% ethanol 75% DCM and 10 mg/mL resveratrol. Arrows delineate the organic droplet against the bottom of the vial.

3.4. Effect of hydroxyl group number and placement on particle morphology

Resveratrol is a *trans*-stilbene derivative where hydroxyl groups reside at the 3, 5, and 4′ positions relative to the double bond (Fig. 4c). We hypothesized that hydroxyl group number and placement would impact particle morphology. Thus, we produced particles with *trans*-stilbene, which has no OH groups, pinosylvin, which lacks the 4′ OH group of resveratrol, and piceatannol, which has an additional OH group at the 3′ position when compared to resveratrol (Fig. 4). We found that incorporation of *trans*-stilbene or pinosylvin into the emulsion resulted in spherical particles. In contrast, incorporation of piceatannol largely inhibited particle formation. The mass yield of particles dropped from 60% (for *trans*-stilbene) to 12% for piceatannol, making it difficult to study the piceatannol particles via microscopy (Fig. 4D). The particles that did form in the presence of piceatannol appeared irregular in shape. We conclude that the degree of hydroxyl substitution impacts emulsion stability. Furthermore, of the *trans*-stilbene derivatives investigated, the number and placement of hydroxyl groups in resveratrol appear to be optimal for inducing crumpled particle morphology at the conditions tested.

3.5. Relative contributions of ethanol and resveratrol on particle morphology

We next investigated the relative contributions of ethanol and resveratrol on particle morphology. Decreasing the resveratrol concentration from 10 mg/mL (used to make the particles depicted in Figs. 1 and 4 C) to 4 mg/mL, while maintaining the ethanol concentration at 25%, led to particles that were mostly spherical; however, we did

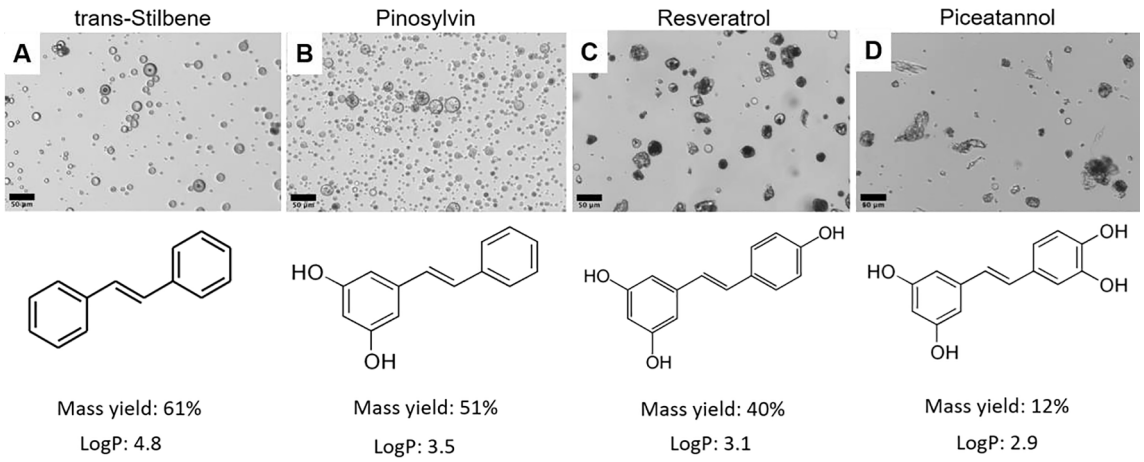

Fig. 4. Effect of resveratrol-like molecules on particle morphology. Particles were made with an organic phase that was 25% ethanol, 75% DCM, and 6% PLG. In addition, the organic phase contained a stilbene at 10 mg/mL. The stilbenes investigated were (A) *trans*-stilbene, (B) pinosylvin, (C) resveratrol, or (D) piceatannol. Light microscopy images are shown along with the stilbene's structure and logP. The mass yield of particles is also listed. Scale bars indicate 50 μm.

observe a small population of particles with crumpled morphology (Fig. 5 A,D, red arrows). Particles made this way had relatively low resveratrol loading, 1.5 μg/mL. Particles made with 25% ethanol, but no resveratrol were spherical, indicating resveratrol is required for particle crumpling (Fig. 5 B,E). Interestingly, when ethanol concentration was decreased to 10% while maintaining resveratrol at 4 mg/mL, particles were also spherical (Fig. 5 C,F) and had a resveratrol loading of 4 mg/mL, which was 2.6-fold higher compared to the conditions in Fig. 5 A,D. The data suggests that resveratrol loading may not be the defining factor that dictates particle morphology and that ethanol may enhance resveratrol's effect on particle buckling and crumpling.

3.6. The effect of cosolvent on particle morphology

Here, we sought to understand the effect of cosolvent on particle morphology. To accomplish this, we fabricated particles using either ethanol, methanol, or acetone as the cosolvent. All three solvents are able to solubilize resveratrol to a similar degree (50 mg/mL, Table 3). One difference between these three solvents is their solubility in water, which is also reflected by their LogP values (Table 3). Specifically, methanol is about twice as soluble in water as acetone, and ethanol's solubility resides in between methanol and acetone. An additional difference is that PLG is soluble in acetone at 6%, but not in ethanol or methanol (Table 3).

Table 3
Solvent Properties (Banerjee, 1984; Riddick et al., 1986; Schneider, 1983).

Solvent	RSV Solubility (mg/mL)	6% PLG solubility	Solubility in Water	LogP
Methanol	50	No	31.21 M	−0.77
Ethanol	50	No	21.71 M	−0.31
Acetone	50	Soluble	17.22 M	−0.24
Ethyl Acetate	10	Soluble	0.91 M	0.73
Dichloromethane	None	Soluble	0.15 M	1.25

Utilizing ethanol as the cosolvent resulted in many highly crumpled particles and some smaller particles that were spherical (Fig. 6A,D). Resveratrol content of the particles made with ethanol was 65 μg/mg. Utilizing methanol as the cosolvent also resulted in crumpled particles and a population of spherical particles that tended to be smaller than the nonspherical particles (Fig. 6B,E). Resveratrol content of particles made with methanol was 50 μg/mg. Finally, when acetone was used as the

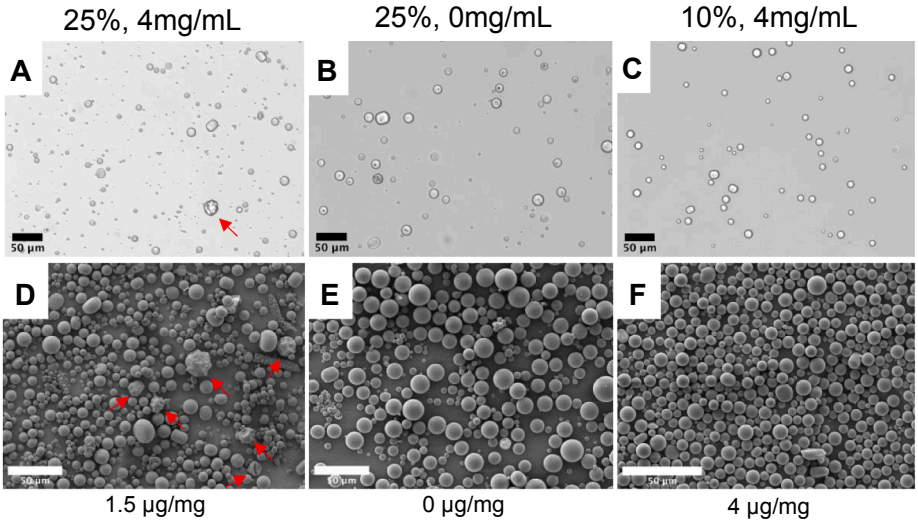

Fig. 5. Relative contributions of ethanol and resveratrol on particle morphology. (A-C) Light microscopy images and (D-F) SEM images of particles made with differing amounts of resveratrol and ethanol in the oil phase. (A,D) 25% ethanol and 4 mg/mL resveratrol, (B,E) 25% ethanol and 0 mg/mL resveratrol, (C,F) 10% ethanol and 4 mg/mL resveratrol. Red arrows indicate crumpled particles. Scale bars indicate 50 μm.

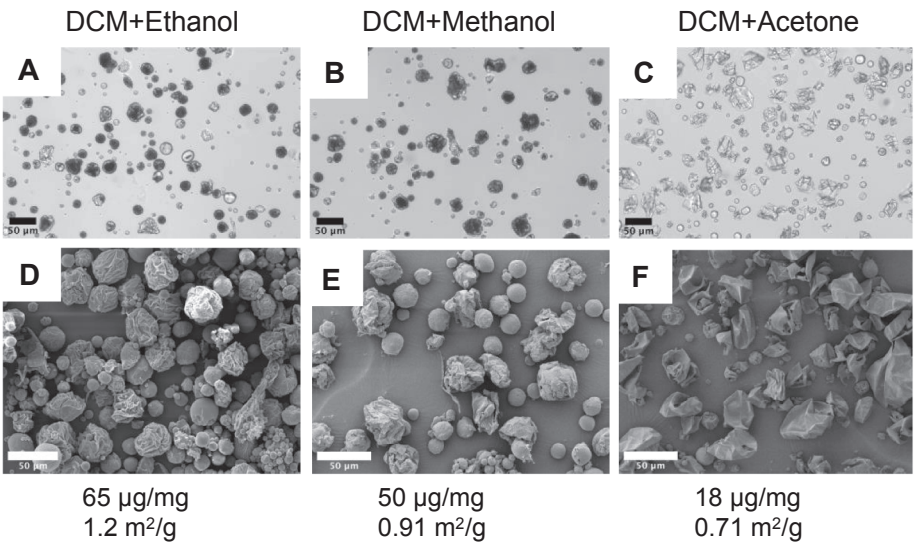

Fig. 6. The effect of cosolvent on particle morphology. Representative images of PLG particles made with organic phases that were: (A,D) 25% ethanol and 75% DCM, (B,E) 25% methanol and 75% DCM, and (C,F) 25% acetone and 75% DCM. (A-C) are light microscopy images and (D-F) are SEM. The oil phase contained 6% PLG and 10 mg/mL RSV. The aqueous phase contained 1% PVA. Scale bars indicate 50 µm. Resveratrol loading is listed for each formulation in µg/mg. Surface area was determined by BET theory applied to Krypton adsorption isotherms and is listed in m^2/g.

cosolvent, particle morphology resembled collapsed spheres, with deep indentations (Fig. 6C,F). Once again, spherical particles were also observed, but they tended to be smaller than the nonspherical particles. Resveratrol content of particles made with acetone was 18 µg/mg. In addition, particles made with methanol or acetone, but without resveratrol, were spherical (data not shown), which was the case when ethanol, but no resveratrol was used (Fig. 1).

To quantify the differences in morphology between the particles formed with the three cosolvents, we calculated surface area using krypton gas adsorption measurements and BET theory. Particles made with ethanol, methanol, and acetone had specific surface areas of 1.2, 0.91, and 0.71 m^2/g, respectively. The data indicates the crumpled morphology achieved with ethanol has 70% higher specific surface area than the collapsed spheres made with acetone. In addition, we find surface area correlates with resveratrol content.

3.7. Effect of ethyl acetate as the organic solvent on particle morphology

The data up to this point led us to hypothesize that the two solvent system involving DCM and a cosolvent was causing nonspherical particle formation. Thus, we searched for a solvent able to solubilize both PLG and resveratrol. We found that resveratrol was soluble up to 10 mg/mL in ethyl acetate containing 6% PLG (Table 3). In addition, ethyl acetate has been used to make PLG particles using PVA as the emulsifier (Sah, 1997). Particles fabricated using ethyl acetate containing the same concentrations of resveratrol (10 mg/mL) and PLG (6%) as the DCM/ethanol system were smooth and spherical instead of crumpled (Fig. 7). Particles made with ethyl acetate had similar loading to the highest loaded particles made with DCM and ethanol (57 µg/mg vs 65 µg/mg), but a lower surface area (0.78 m^2/g vs 1.2 m^2/g). This was expected because the particles made with ethyl acetate were spherical. Thus, we conclude that particle buckling that leads to the crumpled morphology is specific to when particles are made with resveratrol, and DCM is used with a cosolvent.

3.8. Production of nonspherical particles using polycaprolactone and poly (L-lactide)

We were interested if crumpled particles could be produced from other polyesters that have been FDA approved for use in medical devices and drug delivery systems. We found that nonspherical particle formation could be achieved using polycaprolactone (PCL) or poly(L-lactide) (PLLA), which is demonstrated in Fig. 8 A and C. To confirm that resveratrol was required for nonspherical particle formation, we made particles without resveratrol (blank particles) and confirmed they were spherical (Fig. 8 B,D). Interestingly, the PCL particles were larger than the PLLA particles, which were similar in size when compared to PLG particles made without resveratrol. The PCL particles were probably larger because the PCL used has a higher inherent viscosity than the other two polymers and will naturally form larger droplets in the emulsion (Li et al., 2008).

3.9. Incorporation of coumarin 6 into resveratrol loaded particles

One application of nonspherical particles is drug delivery, and we investigated if a hydrophobic agent could be encapsulated in the

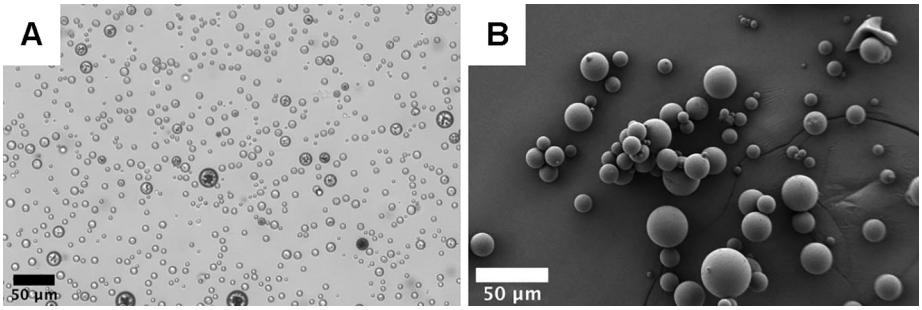

Fig. 7. Effect of Ethyl Acetate on particle morphology. Light microscope (A) and SEM (B) images of resveratrol loaded particles made with ethyl acetate as the organic solvent. The oil phase contained 10 mg/mL resveratrol and 6% PLG. The aqueous phase contained 1% PVA. Resveratrol loading was 57 µg/mg and the surface area was calculated to be 0.78 m^2/g. Scale bars indicate 50 µm.

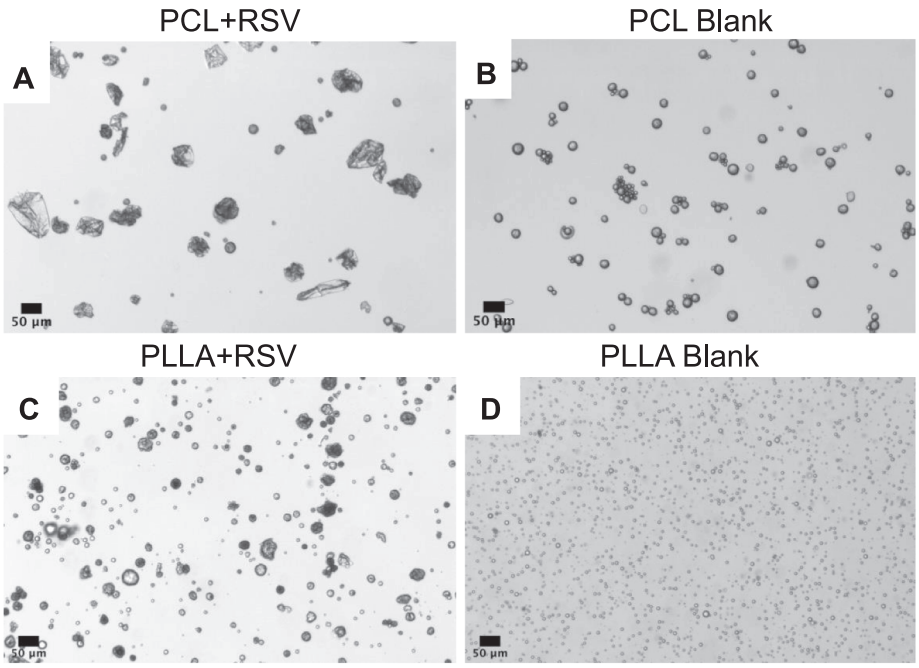

Fig. 8. Morphology of polycaprolactone (PCL) and poly(L-lactide) (PLLA) particles made with resveratrol. Representative images of particles made with an oil phase consisting of (A,C) 25% ethanol and 75% DCM and 10 mg/mL of resveratrol or (B,D) 100% DCM with no resveratrol. (A,B) were made with an oil phase that was 6% PCL and (C,D) were made with an oil phase that was 6% PLLA. The aqueous phase of the emulsion contained 1% PVA. Scale bars indicate 50 μm.

crumpled particles formed with resveratrol. As proof of concept, we added coumarin 6, a hydrophobic fluorochrome, to the oil phase containing ethanol, DCM, PLG and resveratrol. These particles formed with the same crumpled morphology as particles produced without coumarin 6 (compare Fig. 9A with Fig. 6A) and were highly fluorescent (Fig. 9B), indicating coumarin 6 was successfully encapsulated. Encapsulating coumarin 6 in the absence of resveratrol resulted in smooth particles, demonstrating that coumarin 6 does not have an effect on particle morphology (Fig. 9 C,D). These results suggest that hydrophobic bioactive agents could be encapsulated into the crumpled particles for drug delivery applications.

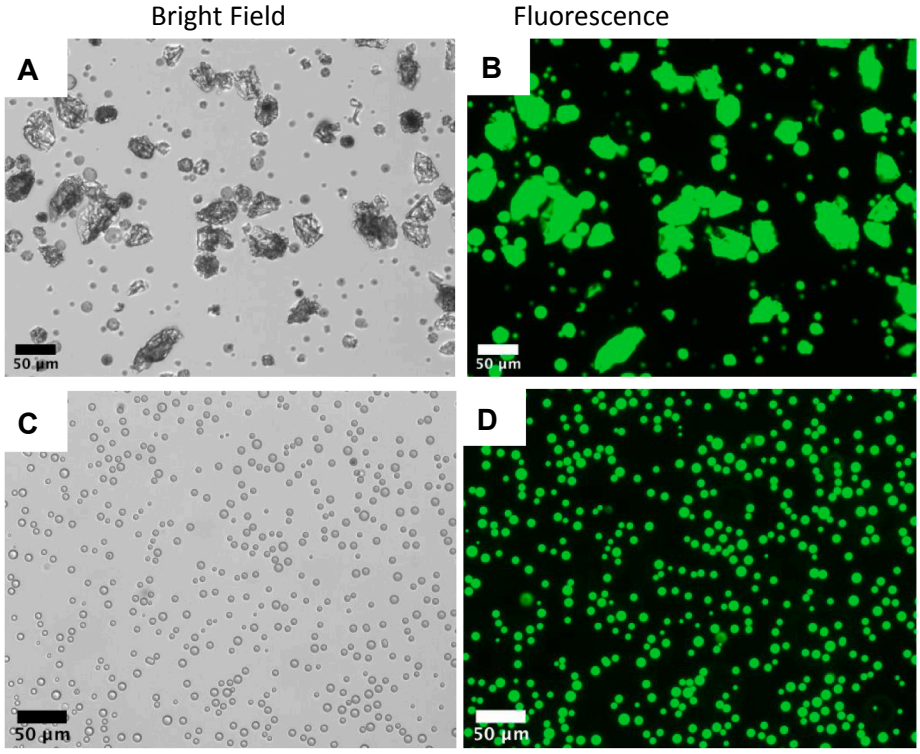

Fig. 9. Coumarin 6 can be encapsulated into crumpled particles formed with resveratrol. Particles were fabricated with an oil phase consisting of 25% ethanol, 75% DCM, 6% PLG, and 0.5 mg/mL coumarin 6 with (A, B) or without (C,D) 10 mg/mL resveratrol. Scale bar indicates 50 μm.

3.10. Separation of nonspherical particles by size

Particle size impacts drug release kinetics (Chen et al., 2017). Size also dictates how a biological system will interact with the particle. For example, particles smaller than 6 μm are readily phagocytosed by macrophages, while larger particles are left to reside in the extracellular space (Veiseh et al., 2015). To demonstrate that nonspherical particles could be sorted based on size, differential centrifugation was employed to separate particles made with 25% ethanol and 75% DCM and 10 mg/mL of resveratrol. The process successfully separated 3 size ranges, as can be seen in Fig. 10. Centrifugation at 1xg collected particles above 25 μm (Fig. 10A). A subsequent round of centrifugation at 30xg collected particles between 6 μm and 25 μm (Fig. 10B). A final round of centrifugation at 250xg collected particles that were less than 6 μm (Fig. 10C). The images suggest that the frequency of crumpled particles may decrease as size decreases.

4. Discussion

The O/W emulsion/solvent extraction technique is a simple and scalable method for producing polymer particles, and has been used in the fabrication of several FDA approved polymer particle therapies (Wischke and Schwendeman, 2008). However, it is challenging to produce particles of nonspherical morphology, as O/W emulsions preferentially produce spherical particles. Here we present a facile method for producing nonspherical PLG particles by adding resveratrol and a cosolvent to the oil phase of a DCM/PLG/PVA/H_2O emulsion. While addition of resveratrol and ethanol produce particles with a "crumpled paper" morphology, addition of resveratrol and acetone produce particles with a morphology that resembles deflated or indented spheres. We demonstrate broad applicability of the technique by producing nonspherical particles out of polycaprolactone and poly(L-lactide) in addition to PLG. Importantly, PCL and PLL are slower degrading polymers compared to PLG. Using polymers with varying degradation times can be used to modulate release rates for drug delivery applications (Hines and Kaplan, 2013). In addition, we co-encapsulate resveratrol with a hydrophobic fluorescent dye, coumarin 6, which produces fluorescent nonspherical particles. This result suggests hydrophobic bioactive agents could be encapsulated into the crumpled particles for drug delivery applications. A previous study co-encapsulated nonspherical particles with fluorescent molecules with a lithography approach (Rolland et al., 2005), but the benefit of our system is that the O/W emulsion/solvent extraction is more scalable. Finally, we show that using differential centrifugation we can purify large particles (>25 μm particles) that could act as drug depots or smaller particles (less than 6 μm) that could be endocytosed for intracellular drug delivery applications (Champion et al., 2008; Kissel et al., 1991).

To our knowledge, no other studies have reported production of crumpled or highly deformed spherical particles using the O/W emulsion/solvent extraction technique (Jindal, 2017). Many nonspherical particles have been produced using microfluidics, photopolymerization and lithography. A wide variety of shapes have been made using these methods such as rods, discs, rings, and wrinkled particles (Champion et al., 2007; Jindal, 2017; Li et al., 2016). These methods have been successful in controlling morphology; however, those fabrication processes are not currently used to make FDA approved controlled release formulations (Wischke and Schwendeman, 2008) and they are less efficient than the O/W emulsion/solvent extraction in terms of making large quantities of particles for industrial purposes.

Video microscopy revealed that addition of resveratrol and ethanol to the dispersed phase of the emulsion caused the spherical droplets to buckle as they decreased in volume leading to a crumpled morphology. Generally, droplets in these emulsions (i.e. DCM/PLG/PVA/H_2O) remain spherical up until the polymers precipitate and the particle forms. This is likely because there is sufficient mobility for the polymer chains to reorganize and condense as droplet volume deceases (due to diffusion of DCM out of the droplet). The buckling behavior observed when resveratrol and ethanol are added to the emulsion is reminiscent of when a thin, spherical elastic shell is deformed by applying external pressure or reducing the volume (Vliegenthart and Gompper, 2011). This phenomenon can be visualized with a ping pong ball. When pressed on at a single location, with sufficient force, the shell indents. If the ball is pressed on at multiple points with sufficient force, the shell crumples with multiple indentations. It is unclear why the emulsion droplets crumple with the addition of resveratrol and ethanol. The literature is rich with reports of encapsulating small molecules in PLG particles (Berkland et al., 2003; Chen et al., 2017; Dawes et al., 2009; Raman et al., 2005) and, to our knowledge, crumpled morphology was not observed, even when ethanol was added to a DCM/PLG/PVA/H_2O emulsion used to encapsulate dexamethasone (Rawat and Burgess, 2010). It does appear that the hydroxyl groups are optimally positioned on resveratrol to induce the crumpled morphology because switching out resveratrol for pinosylvin, which lacks the 4′ hydroxyl group, led to spherical particles, while using piceatannol with the additional 3′ hydroxyl decreased particle yield to 12%, indicating particle formation was disrupted in some way. We think that resveratrol somehow restricts chain motion of the polymers at the oil–water interface. The reduction in their fluidity would introduce a shear modulus that could lead to buckling behavior as the droplet decreases in volume (Witten, 2007). XRD of the highly crumpled particles suggest that there may be small amounts of crystalline resveratrol. Perhaps these crystalline regions form at the oil–water interface during solvent extraction and restrict polymer chain motion as the droplet shrinks. In support of this idea, a white precipitate is seen forming at the oil water interface in the sessile drop experiment. Another possibility is that resveratrol molecules, rather than crystals, restrict chain motion during droplet shrinkage. We propose that resveratrol might accomplish this by hydrogen bonding with carbonyl groups in the PVA.

Cosolvent appears to play an important role in resveratrol-induced particle crumpling. We believe this role is to transport resveratrol to the oil–water interface. Addition of resveratrol to the DCM/PLG/PVA/H_2O emulsion with the aid of ethanol, methanol, or acetone all led to particle crumpling (albeit varying degrees, discussed below). In contrast, when ethyl acetate was used instead of DCM, a cosolvent was not needed and particles remained spherical. Furthermore, there is a dose dependence of cosolvent on particle crumpling. When the oil phase contained 10% ethanol and 4 mg/mL resveratrol, only spherical particles were observed; however, when ethanol was increased to 25%,

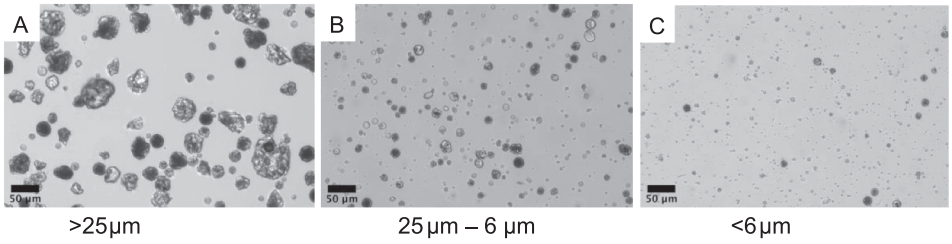

Fig. 10. Nonspherical particles can be separated by size using differential centrifugation. Particles were fabricated with an oil phase consisting of 25% ethanol, 75% DCM 6% PLG, and 10 mg/mL resveratrol. The aqueous phase was 1% PVA. Particles were separated by size using differential centrifugation. Particles were first centrifuged at 1xg (A), then at 30xg (B), and finally at 250xg (C) each for 10 min. These steps produced particles that were 25 μm and greater (A), 25 μm – 6 μm (B), and less than 6 μm (C).

particle crumpling was detected in a small population of particles. We propose that as the cosolvent leaves the droplet, some portion of the resveratrol is redistributed from the bulk of the droplet to the surface, and greater redistribution is achieved by increasing cosolvent concentration. Interestingly, particles made with 25% ethanol, which exhibited a low frequency of particle crumpling, contained less resveratrol (2.5x less) than the those made with 10% ethanol. It is tempting to conclude that resveratrol content and particle crumpling can be decoupled as long as sufficient resveratrol is transported to the oil-water interface. However, we caution that the resveratrol measurements are an average value for the entire batch of particles and may not reflect the true loading of the small population of crumpled particles, which could have much higher resveratrol content than the smooth particles.

The cosolvent used had a dramatic effect on particle morphology in some cases. By switching out ethanol for acetone we produced particles resembling deflated spheres with few, large indentations rather than spheres that were highly crumpled. The shape of a deformed thin spherical shell, which can vary from a sphere with a single indentation to sphere with many indentations, which appears highly crumpled, depends on deformation rate, extent of volume change, and the Föppl-von Kármán (FvK) number (Vliegenthart and Gompper, 2011). The FvK number is the ratio of shell radius to shell thickness scaled by Poisson's ratio. Essentially, shells with a larger FvK deform more readily and, thus, require a smaller volume change in order to deform. Modeling indicates that for a given FvK and volume change, a large deformation rate leads to the simultaneous formation of many indentations that culminate in a high degree of crumpling, while a sufficiently slow deformation rate results in a single indentation (Vliegenthart and Gompper, 2011). In fact, the modeling suggests there is a lower limit on deformation rate that must be achieved otherwise only 1 or 2 indentations result (Vliegenthart and Gompper, 2011), and the morphology resembles that of the particles made with acetone. We propose that deformation rate (i.e. change in droplet volume) may be different for droplets formed with ethanol versus acetone because ethanol has a higher solubility in water (Table 3) and could possibly leave the droplet faster. Following this logic, using ethanol as a co-solvent leads to droplet deformation rates that support multiple indentations and a highly crumpled surface when the particle forms, while using acetone leads to relatively slower deformation rates that cause fewer indentations and a deflated sphere morphology.

The hypothesis that crumpled particle morphology correlates with cosolvent solubility with water is not supported by the methanol data. Indeed, methanol is more soluble in water than ethanol or acetone. Furthermore, the difference in water solubility is actually greater between methanol and ethanol than ethanol and acetone (Table 3). Despite this, particles made with methanol had less surface area compared to particles made by ethanol, indicating they were less crumpled or there was a lower frequency of droplets that crumpled. Thus, factors other than cosolvent miscibility with water must also be important in determining particle morphology. We found that surface area correlates with resveratrol content among the particles made with the three different cosolvents. Particles made with ethanol had a resveratrol content of 65 μg/mg and a surface area of 1.2 m^2/g. Particles made with methanol contained 23% less resveratrol and had a corresponding 25% decrease in surface area compared to the particles made with ethanol. However, particles made with acetone contained 72% less resveratrol than those made with ethanol but exhibited only a 40% decrease in surface area. We believe this data indicates that some cosolvents are better at transporting and/or retaining resveratrol at the oil–water interface at critical levels that support droplet deformation as it shrinks, with both ethanol and acetone outperforming methanol in this regard.

Many of the nonspherical particles observed were greater than 20 μm in size, ranging up to almost 50 μm. Potential biomedical applications for particles in this size range include acting as a drug depot or acting as a matrix for cell attachment and growth. PLG microspheres loaded with naltrexone have been FDA approved, and have an average diameter around 60 μm (Andhariya et al., 2017). The naltrexone particles are smooth and spherical and provide nearly a zero-order release profile over 4 weeks. It is established that particle morphology impacts drug release (Jindal, 2017). While it is unknown how the morphologies produced herein would impact drug release profiles, we expect that drug release would be increased (compared to spherical particles with similar size and drug loading) due to increased surface area. It has also been reported that 40 μm particles with wrinkled surfaces promote greater cell adhesion, when used as matrices for fibroblast culture, compared to smooth particles (Li et al., 2016). Thus, crumpled drug delivery depots might be leveraged to target cell populations in tissues based on their propensity to adhere to the crumpled surface.

Intracellular delivery of bioactive factors is an important aspect of drug delivery, especially when modulating the immune system (Liu et al., 2019; Shae et al., 2019; Son et al., 2020; Zhang et al., 2019). While many of the nonspherical particles produced herein are too large for endocytosis, we believe that the emulsion conditions can be modified to produce smaller, nonspherical particles with ridges and flat surfaces that might impact cell uptake and intracellular delivery of bioactive factors. For example, decreasing polymer molecular weight and increasing homogenization speeds produces smaller droplets that will condense into smaller particles (Li et al., 2008). However, it is important to consider that the small particles were less likely to be crumpled or indented in the present work. This was not surprising because smaller droplets have a smaller FvK number and thus are more resistant to crumpling (Vliegenthart and Gompper, 2011). The resistance of small droplets to crumpling has also been reported for Pickering emulsions, in which the droplet surface is solid (Datta et al., 2010). For thin, elastic shells with small FvK numbers, slow deformation rates were more effective at producing indentations (Vliegenthart and Gompper, 2011). Thus, focusing on acetone as the cosolvent may be a promising avenue to develop small, nonspherical particles for intracellular drug delivery.

A final consideration is the effect of resveratrol delivery from the particle, since it is required to modulate particle shape. When given orally, resveratrol has been found to be an antioxidant (de la Lastra and Villegas, 2007), anti-inflammatory (De la Lastra and Villegas, 2005), or an exercise mimetic (Baur and Sinclair, 2006). Resveratrol is available as a supplement in pill form and high doses (150 mg, six times/day, for thirteen doses) were well tolerated in a clinical trial (Almeida et al., 2009). In vitro, it is found that concentrations of 50–100 μM do not induce toxicity while inducing lipid mobilization in adipocytes and downregulation of inflammatory signaling in macrophages (Cullberg et al., 2014; Picard et al., 2004). For comparison, if 1 mg of the highly crumpled particles (resveratrol loading of 65 μg/mg) released their resveratrol content into 100 mL of water (or tissue) instantaneously, the concentration would be less than 3 μM. Thus, while resveratrol toxicity would need to be investigated for each biological system in which the particles were applied, we believe it is plausible the resveratrol would be well tolerated and could possibly synergize with other drug payloads. In addition, resveratrol can also act as a preservative and increases the stability of a-tocopherol encapsulated in whey protein particles subjected to oxidizing conditions (Wang et al., 2016). However, if resveratrol loading is undesirable, our previous research demonstrates we can decrease loading by up to 60% with a 1-minute ethanol wash (Isely et al., 2019). How this wash affects the loading of other bioactive factors will need to be carefully studied as we move this technology forward.

5. Conclusion

Addition of resveratrol, with the aid of a cosolvent, to an emulsion of dichloromethane and poly(lactide-co-glycolide) in aqueous polyvinyl alcohol leads to the production of nonspherical particles following solvent extraction. Particle shape can be modulated by cosolvent type with ethanol yielding highly crumpled particles and acetone leading to particles that resemble deflated spheres. In addition, spherical particles can be obtained if ethyl acetate is used in lieu of dichloromethane and a

cosolvent. The method extends to polycaprolactone and poly(L-lactic acid) and is compatible with the encapsulation of a hydrophobic fluorescent dye, suggesting hydrophobic bioactive agents could be encapsulated. Video microscopy revealed that oil droplets crumple as they decrease in volume during solvent extraction when resveratrol and ethanol were present. Crumpling did not occur when droplets contained ethanol without resveratrol and geometry remained spherical until the particles formed. This crumpling behavior is similar to when a thin elastic shell is deformed and suggests that the surface of the droplets containing ethanol and resveratrol may not be sufficiently fluid to maintain a spherical morphology as the droplet decreases in volume. Resveratrol's hydroxyl groups appear to be optimally positioned to induce the non-spherical particles because the crumpling is lost with the removal of the 4′ hydroxyl group or the addition of a 3′ hydroxyl group. Based on all the data, we propose that resveratrol inhibits chain motion of polymers at the droplet's surface that must reorganize in order to maintain a spherical geometry and the function of the cosolvent is to redistribute resveratrol from the droplet's bulk to its surface. To our knowledge, no other studies have reported production of crumpled or highly deformed spherical particles using the oil in water emulsion/solvent extraction technique. Since particle morphology impacts drug release kinetics and how biological systems engage with a biomaterial, this method could be used to fine-tune FDA approved polymer-based controlled release therapies already on the market or enable the development of novel particle based systems to control or study cell biology.

Funding

This work was supported in part by NIH grants P20GM103641 and P20GM109091 and U.S. Department of Veterans Affairs grant I21RX003191.

CRediT authorship contribution statement

Christopher Isely: Conceptualization, Methodology, Validation, Investigation, Formal analysis, Writing - original draft, Visualization. **Alexandra C. Stevens:** Investigation, Formal analysis. **Gregory L. Tate:** Methodology, Investigation, Formal analysis. **John R. Monnier:** Methodology, Investigation, Formal analysis, Resources. **R. Michael Gower:** Conceptualization, Methodology, Formal analysis, Resources, Writing - original draft, Writing - review & editing, Visualization, Supervision, Funding acquisition.

Declaration of Competing Interest

The authors declare that they have no known competing financial interests or personal relationships that could have appeared to influence the work reported in this paper.

Acknowledgements

We thank the Lauterbach Group for use of their XRD instrument.

References

Almeida, L., Vaz-da-Silva, M., Falcão, A., Soares, E., Costa, R., Loureiro, A.I., Fernandes-Lopes, C., Rocha, J.-F., Nunes, T., Wright, L., Soares-da-Silva, P., 2009. Pharmacokinetic and safety profile of trans-resveratrol in a rising multiple-dose study in healthy volunteers. Mol. Nutr. Food Res. 53, S7–S15. https://doi.org/10.1002/mnfr.200800177.

Andhariya, J.V., Shen, J., Choi, S., Wang, Y., Zou, Y., Burgess, D.J., 2017. Development of in vitro-in vivo correlation of parenteral naltrexone loaded polymeric microspheres. J. Controlled Release 255, 27–35. https://doi.org/10.1016/j.jconrel.2017.03.396.

Banerjee, A., Qi, J., Gogoi, R., Wong, J., Mitragotri, S., 2016. Role of nanoparticle size, shape and surface chemistry in oral drug delivery. J. Controlled Release 238, 176–185. https://doi.org/10.1016/j.jconrel.2016.07.051.

Banerjee, Sujit, 1984. Solubility of organic mixtures in water. Environ. Sci. Technol. 18, 587–591. https://doi.org/10.1021/es00126a004.

Baur, J.A., Sinclair, D.A., 2006. Therapeutic potential of resveratrol: the in vivo evidence. Nat. Rev. Drug Discov. 5, 493–506. https://doi.org/10.1038/nrd2060.

Berkland, C., Kim, K., Pack, D.W., 2003. PLG Microsphere Size Controls Drug Release Rate Through Several Competing Factors. Pharm. Res. 20, 1055–1062. https://doi.org/10.1023/A:1024466407849.

Brunauer, S., Emmett, P.H., Teller, E., 1938. Adsorption of Gases in Multimolecular Layers. J. Am. Chem. Soc. 60, 309–319. https://doi.org/10.1021/ja01269a023.

Champion, J.A., Katare, Y.K., Mitragotri, S., 2007. Particle shape: A new design parameter for micro- and nanoscale drug delivery carriers. J. Controlled Release 121, 3–9. https://doi.org/10.1016/j.jconrel.2007.03.022.

Champion, J.A., Mitragotri, S., 2006. Role of target geometry in phagocytosis. Proc. Natl. Acad. Sci. 103, 4930–4934. https://doi.org/10.1073/pnas.0600997103.

Champion, J.A., Walker, A., Mitragotri, S., 2008. Role of Particle Size in Phagocytosis of Polymeric Microspheres. Pharm. Res. 25, 1815–1821. https://doi.org/10.1007/s11095-008-9562-y.

Chen, W., Palazzo, A., Hennink, W.E., Kok, R.J., 2017. Effect of Particle Size on Drug Loading and Release Kinetics of Gefitinib-Loaded PLGA Microspheres. Mol. Pharm. 14, 459–467. https://doi.org/10.1021/acs.molpharmaceut.6b00896.

Cullberg, K.B., Foldager, C.B., Lind, M., Richelsen, B., Pedersen, S.B., 2014. Inhibitory effects of resveratrol on hypoxia-induced inflammation in 3T3-L1 adipocytes and macrophages. J. Funct. Foods 7, 171–179. https://doi.org/10.1016/j.jff.2014.02.015.

Datta, S.S., Shum, H.C., Weitz, D.A., 2010. Controlled Buckling and Crumpling of Nanoparticle-Coated Droplets. Langmuir 26, 18612–18616. https://doi.org/10.1021/la103874z.

Dawes, G.J.S., Fratila-Apachitei, L.E., Mulia, K., Apachitei, I., Witkamp, G.-J., Duszczyk, J., 2009. Size effect of PLGA spheres on drug loading efficiency and release profiles. J. Mater. Sci. Mater. Med. 20, 1089–1094. https://doi.org/10.1007/s10856-008-3666-0.

De la Lastra, C.A., Villegas, I., 2005. Resveratrol as an anti-inflammatory and anti-aging agent: Mechanisms and clinical implications. Mol. Nutr. Food Res. 49, 405–430. https://doi.org/10.1002/mnfr.200500022.

de la Lastra, C.A., Villegas, I., 2007. Resveratrol as an antioxidant and pro-oxidant agent: mechanisms and clinical implications. Biochem. Soc. Trans. 35, 1156–1160. https://doi.org/10.1042/BST0351156.

Hines, D.J., Kaplan, D.L., 2013. Poly(lactic-co-glycolic) Acid-Controlled-Release Systems: Experimental and Modeling Insights. Crit. Rev. Ther. Drug Carrier Syst. 30, 257–276. https://doi.org/10.1615/CritRevTherDrugCarrierSyst.2013006475.

Hussain, M., Xie, J., Wang, K., Wang, H., Tan, Z., Liu, Q., Geng, Z., Shezad, K., Noureen, L., Jiang, H., Xu, J., Zhang, L., Zhu, J., 2019. Biodegradable Polymer Microparticles with Tunable Shapes and Surface Textures for Enhancement of Dendritic Cell Maturation. ACS Appl. Mater. Interfaces 11, 42734–42743. https://doi.org/10.1021/acsami.9b14286.

Isely, C., Hendley, M.A., Murphy, K.P., Kader, S., Annamalai, P., Gower, R.M., 2019. Development of microparticles for controlled release of resveratrol to adipose tissue and the impact of drug loading on particle morphology and drug release. Int. J. Pharm. 568, 118469 https://doi.org/10.1016/j.ijpharm.2019.118469.

Jindal, A.B., 2017. The effect of particle shape on cellular interaction and drug delivery applications of micro- and nanoparticles. Int. J. Pharm. 532, 450–465. https://doi.org/10.1016/j.ijpharm.2017.09.028.

Kissel, T., Brich, Z., Bantle, S., Lancranjan, I., Nimmerfall, F., Vit, P., 1991. Parenteral depot-systems on the basis of biodegradable polyesters. J. Controlled Release 16, 27–41. https://doi.org/10.1016/0168-3659(91)90028-C.

Lee, B.K., Yun, Y., Park, K., 2016. PLA micro- and nano-particles. Adv. Drug Deliv. Rev. 107, 176–191. https://doi.org/10.1016/j.addr.2016.05.020.

Li, M., Joung, D., Hughes, B., Waldman, S.D., Kozinski, J.A., Hwang, D.K., 2016. Wrinkling Non-Spherical Particles and Its Application in Cell Attachment Promotion. Sci. Rep. 6, 30463. https://doi.org/10.1038/srep30463.

Li, M., Rouaud, O., Poncelet, D., 2008. Microencapsulation by solvent evaporation: State of the art for process engineering approaches. Int. J. Pharm. 363, 26–39.

Liu, Q., Wang, X., Liu, X., Kumar, S., Gochman, G., Ji, Y., Liao, Y.-P., Chang, C.H., Situ, W., Lu, J., Jiang, J., Mei, K.-C., Meng, H., Xia, T., Nel, A.E., 2019. Use of Polymeric Nanoparticle Platform Targeting the Liver To Induce Treg-Mediated Antigen-Specific Immune Tolerance in a Pulmonary Allergen Sensitization Model. ACS Nano 13, 4778–4794. https://doi.org/10.1021/acsnano.9b01444.

Liu, S., Deng, R., Li, W., Zhu, J., 2012. Polymer Microparticles with Controllable Surface Textures Generated through Interfacial Instabilities of Emulsion Droplets. Adv. Funct. Mater. 22, 1692–1697. https://doi.org/10.1002/adfm.201103018.

Mitragotri, S., 2009. In Drug Delivery, Shape Does Matter. Pharm. Res. 26, 232–234. https://doi.org/10.1007/s11095-008-9740-y.

Mohamed, F., van der Walle, C.F., 2006. PLGA microcapsules with novel dimpled surfaces for pulmonary delivery of DNA. Int. J. Pharm. 311, 97–107. https://doi.org/10.1016/j.ijpharm.2005.12.016.

Murphy, K.P., Hendley, M.A., Isely, C., Annamalai, P., Peña, E., Gower, R.M., 2018. Resveratrol Delivery from Porous Poly(lactide- *co* -glycolide) Scaffolds Promotes an Anti-Inflammatory Environment within Visceral Adipose Tissue. ACS Appl. Mater. Interfaces 10. https://doi.org/10.1021/acsami.8b13421.

Ogawa, Y., Yamamoto, M., Okada, H., Yashiki, T., Shimamoto, T., 1988. A new technique to efficiently entrap leuprolide acetate into microcapsules of polylactic acid or copoly(lactic/glycolic) acid. Chem. Pharm. Bull. (Tokyo) 36, 1095–1103. https://doi.org/10.1248/cpb.36.1095.

Park, K., Skidmore, S., Hadar, J., Garner, J., Park, H., Otte, A., Soh, B.K., Yoon, G., Yu, D., Yun, Y., Lee, B.K., Jiang, X., Wang, Y., 2019. Injectable, long-acting PLGA formulations: Analyzing PLGA and understanding microparticle formation. J. Controlled Release 304, 125–134. https://doi.org/10.1016/j.jconrel.2019.05.003.

Picard, F., Kurtev, M., Chung, N., Topark-Ngarm, A., Senawong, T., Machado de Oliveira, R., Leid, M., McBurney, M.W., Guarente, L., 2004. Sirt1 promotes fat mobilization in white adipocytes by repressing PPAR-γ. Nature 429, 771–776. https://doi.org/10.1038/nature02583.

Raman, C., Berkland, C., Kevin, K., Pack, D.W., 2005. Modeling small-molecule release from PLG microspheres : effects of polymer degradation and nonuniform drug distribution. 103, 149–158. http://doi.org/10.1016/j.jconrel.2004.11.012.

Rawat, A., Burgess, D.J., 2010. Effect of ethanol as a processing co-solvent on the PLGA microsphere characteristics. Int. J. Pharm. 394, 99–105. https://doi.org/10.1016/j.ijpharm.2010.05.013.

Riddick, J.A., Bunger, W.B., Sakano, T., Weissberger, A., 1986. Organic solvents: physical properties and methods of purification, 4th, ed. ed. Techniques of chemistry, Wiley, New York.

Rolland, J.P., Maynor, B.W., Euliss, L.E., Exner, A.E., Denison, G.M., DeSimone, J.M., 2005. Direct Fabrication and Harvesting of Monodisperse, Shape-Specific Nanobiomaterials. J. Am. Chem. Soc. 127, 10096–10100. https://doi.org/10.1021/ja051977c.

Rotenberg, Y., Boruvka, L., Neumann, A.W., 1983. Determination of surface tension and contact angle from the shapes of axisymmetric fluid interfaces. J. Colloid Interface Sci. 93, 169–183. https://doi.org/10.1016/0021-9797(83)90396-X.

Sah, H., 1997. Microencapsulation techniques using ethyl acetate as a dispersed solvent: effects of its extraction rate on the characteristics of PLGA microspheres. J. Controlled Release 47, 233–245. https://doi.org/10.1016/S0168-3659(97)01647-7.

Schneider, G.M., 1983. A. L. Horvath: Halogenated Hydrocarbons. Solubility - Miscibility with Water, Marcel Dekker Inc, New York, Basel 1982. 889 Seiten, Preis: 310 SFr. Berichte Bunsenges. Für Phys. Chem. 87, 289. https://doi.org/10.1002/bbpc.19830870329.

Shae, D., Becker, K.W., Christov, P., Yun, D.S., Lytton-Jean, A.K.R., Sevimli, S., Ascano, M., Kelley, M., Johnson, D.B., Balko, J.M., Wilson, J.T., 2019. Endosomolytic polymersomes increase the activity of cyclic dinucleotide STING agonists to enhance cancer immunotherapy. Nat. Nanotechnol. 14, 269–278. https://doi.org/10.1038/s41565-018-0342-5.

Son, S., Nam, J., Zenkov, I., Ochyl, L.J., Xu, Y., Scheetz, L., Shi, J., Farokhzad, O.C., Moon, J.J., 2020. Sugar-Nanocapsules Imprinted with Microbial Molecular Patterns for mRNA Vaccination. Nano Lett. 20, 1499–1509. https://doi.org/10.1021/acs.nanolett.9b03483.

Su, Z.-X., Shi, Y.-N., Teng, L.-S., Li, X., Wang, L., Meng, Q.-F., Teng, L.-R., Li, Y.-X., 2011. Biodegradable poly(D, L-lactide-co-glycolide) (PLGA) microspheres for sustained release of risperidone: Zero-order release formulation. Pharm. Dev. Technol. 16, 377–384. https://doi.org/10.3109/10837451003739297.

Syed, Y.Y., Keating, G.M., 2013. Extended-Release Intramuscular Naltrexone (VIVITROL®): A Review of Its Use in the Prevention of Relapse to Opioid Dependence in Detoxified Patients. CNS Drugs 27, 851–861. https://doi.org/10.1007/s40263-013-0110-x.

Ulery, B.D., Nair, L.S., Laurencin, C.T., 2011. Biomedical applications of biodegradable polymers. J. Polym. Sci. Part B Polym. Phys. 49, 832–864. https://doi.org/10.1002/polb.22259.

Veiseh, O., Doloff, J.C., Ma, M., Vegas, A.J., Tam, H.H., Bader, A.R., Li, J., Langan, E., Wyckoff, J., Loo, W.S., Jhunjhunwala, S., Chiu, A., Siebert, S., Tang, K., Hollister-Lock, J., Aresta-Dasilva, S., Bochenek, M., Mendoza-Elias, J., Wang, Y., Qi, M., Lavin, D.M., Chen, M., Dholakia, N., Thakrar, R., Lacík, I., Weir, G.C., Oberholzer, J., Greiner, D.L., Langer, R., Anderson, D.G., 2015. Size- and shape-dependent foreign body immune response to materials implanted in rodents and non-human primates. Nat. Mater. 14, 643–651. https://doi.org/10.1038/nmat4290.

Vliegenthart, G.A., Gompper, G., 2011. Compression, crumpling and collapse of spherical shells and capsules. New J. Phys. 13, 045020 https://doi.org/10.1088/1367-2630/13/4/045020.

Wang, L., Gao, Y., Li, J., Subirade, M., Song, Y., Liang, L., 2016. Effect of resveratrol or ascorbic acid on the stability of α-tocopherol in O/W emulsions stabilized by whey protein isolate: Simultaneous encapsulation of the vitamin and the protective antioxidant. Food Chem. 196, 466–474. https://doi.org/10.1016/j.foodchem.2015.09.071.

Wischke, C., Schwendeman, S.P., 2008. Principles of encapsulating hydrophobic drugs in PLA/PLGA microparticles. Int. J. Pharm. 364, 298–327. https://doi.org/10.1016/j.ijpharm.2008.04.042.

Witten, T.A., 2007. Stress focusing in elastic sheets. Rev. Mod. Phys. 79, 643–675. https://doi.org/10.1103/RevModPhys.79.643.

Wojdyr, M., 2010. *Fityk* : a general-purpose peak fitting program. J. Appl. Crystallogr. 43, 1126–1128. https://doi.org/10.1107/S0021889810030499.

Zhang, F., Parayath, N.N., Ene, C.I., Stephan, S.B., Koehne, A.L., Coon, M.E., Holland, E.C., Stephan, M.T., 2019. Genetic programming of macrophages to perform anti-tumor functions using targeted mRNA nanocarriers. Nat. Commun. 10, 3974. https://doi.org/10.1038/s41467-019-11911-5.